

Characteristics of the Wairau and Awatere faults

The Wairau and Awatere faults are principal faults within the Marlborough Fault System (MFS), a system of mainly right-lateral strike-slip faults that accommodate relative Pacific–Australian plate motion between the Hikurangi subduction margin to the north, and the Alpine right-lateral–reverse oblique-slip fault to the south. From the NE corner of the conspicuous Alpine–Wairau restraining bend (-42.0655° 172.4166°) to the NE-most onshore extent of the fault (-41.4375° 174.0307°), the average strike of the Wairau fault is $\sim 065^{\circ}$. At the Branch River site (between -41.6744° 173.1843° and -41.6686° 173.1996°), the average strike of the Wairau fault is $\sim 064^{\circ}$. From its approximate junction with the Alpine fault (-42.3332° , 172.2610°) to its junction with the eastern Awatere fault near Molesworth Station (-42.0297° 173.3351°), the western (Molesworth) section of the Awatere fault has an average strike of $\sim 070^{\circ}$. At the Saxton River site (between -42.0911° 173.1517° and -42.0879° 173.1654°) the average strike of the Awatere fault is $\sim 074^{\circ}$. The regional and local (site-specific) strikes of the Wairau and Awatere faults are therefore within $\sim 10^{\circ}$ of the Pacific plate motion vector relative to the Australian within the MFS, which is ~ 39 mm/yr at $\sim 253^{\circ}$ (DeMets et al., 1990; DeMets et al., 1994).

The Wairau and Awatere faults are hosted in similar bedrock. The Wairau fault at Branch River juxtaposes sandstone and siltstone greywacke of the Caples terrane, N of the fault, against deformed sandstone and mudstone of the Torlesse composite terrane, S of the fault (Bishop et al., 1976; Rattenbury et al., 2006). The Awatere fault at Saxton River is hosted within the sandstones and mudstones of the Torlesse composite terrane (see also DR2; Rattenbury et al., 2006).

Additionally, these faults have similar average slip rates since ~ 15 – 18 ka, roughly the time of deposition of the oldest terrace deposits at each site (e.g., Lensen, 1968; Mason et al., 2006b). The Wairau fault has a horizontal slip rate of 3 – 5 mm/yr since ~ 18 ka, as determined from measuring displaced features dated using cobble weathering-rind age analysis (Knuepfer, 1988, 1992) or correlated to glacial outwash deposits dating to c. 18 ka (Lensen, 1976). Mason et al. (2006b) reported an average slip rate 5.6 ± 0.8 mm/yr for the Awatere fault, though their data suggest that the slip rate has been highly variable since ~ 15 ka, ranging from as slow as 3.8 ($+1.3$ -1.2) mm/yr between ~ 2 – 4 ka, to as fast as 7.8 ($+2$ -2.4) mm/yr between ~ 5.5 – 7 ka, and (Mason et al., 2006b).

The Wairau and Awatere faults have experienced a similar number of earthquakes since c. 18 ka, with similar amounts of average slip per earthquake. Onshore and offshore paleoseismic records indicate that the Wairau fault has ruptured up to 8 times since c. 18 ka (Zachariasen et al., 2006; Barnes and Pondard, 2010). Paleoseismic trenching at multiple locations along the Awatere fault indicate that the Molesworth section of the Awatere fault has ruptured at least 10 times since c. 13 ka (e.g., McCalpin, 1996; Benson et al., 2001; Mason, 2004; Mason et al., 2006a). Lensen (1968, 1976) used geomorphic features variably displaced ~ 5 – 70 m along the Wairau fault to infer an average slip per event of 5 – 7 m since c. 18 ka. Various workers (e.g., Grapes et al., 1998; Little et al., 1998; Mason and Little, 2006) used offset geomorphic features along the Awatere fault to infer an average slip per event of 5 – 8 m.

Moreover, these findings indicate that the Wairau and Awatere faults have similar tectonic settings, bedrock lithologies, modern slip rates, and number of earthquakes and average slip per event (since ~15–18 ka). Because of these similarities, and the similarities of the Branch River and Saxton River sites discussed in the main text, the Wairau and Awatere faults are comparable for the analyses conducted in this study.

References cited:

Barnes, P. M., and Pondard, N. (2010). Derivation of direct on-fault submarine paleoearthquake records from high-resolution seismic reflection profiles: Wairau Fault, New Zealand. *Geochemistry, Geophysics, Geosystems*, 11. Doi:Artn Q11013 10.1029/2010gc003254.

Benson, A. M., Little, T. A., Van Dissen, R. J., Hill, N., and Townsend, D. B. (2001). Late Quaternary paleoseismic history and surface rupture characteristics of the eastern Awatere strike-slip fault, New Zealand. *Geological Society of America Bulletin*, 113(8), 1079-1091. Doi: 10.1130/0016-7606(2001)113<1079:Lqphas>2.0.Co;2.

Bishop, D. G., Bradshaw, J. D., Landis, C. A., and Turnbull, I. M. (1976). Lithostratigraphy and structure of the Caples terrane of the Humboldt Mountains, New Zealand. *New Zealand Journal of Geology and Geophysics*, 19(6), 827-848.

DeMets, C., Gordon, R. G., Argus, D. F., and Stein, S. (1990). Current Plate Motions. *Geophysical Journal International*, 101(2), 425-478. Doi: 10.1111/j.1365-246X.1990.tb06579.x.

DeMets, C., Gordon, R. G., Argus, D. F., and Stein, S. (1994). Effect of Recent Revisions to the Geomagnetic Reversal Time-Scale on Estimates of Current Plate Motions. *Geophysical Research Letters*, 21(20), 2191-2194. Doi: 10.1029/94gl02118.

Grapes, R., Little, T., and Downes, G. (1998). Rupturing of the Awatere Fault during the 1848 October 16 Marlborough earthquake, New Zealand: historical and present day evidence. *New Zealand Journal of Geology and Geophysics*, 41, 387-399.

Knuepfer, P. L. K. (1988). Estimating Ages of Late Quaternary Stream Terraces from Analysis of Weathering Rinds and Soils. *Geological Society of America Bulletin*, 100(8), 1224-1236. Doi: 10.1130/0016-7606(1988)100<1224:Eaolqs>2.3.Co;2.

Knuepfer, P. L. K. (1992). Temporal Variations in Latest Quaternary Slip across the Australian-Pacific Plate Boundary, Northeastern South Island, New Zealand, *Tectonics*, 11(3), 449-464. Doi: 10.1029/91tc02890.

Lensen, G. J. (1968). Analysis of Progressive Fault Displacement During Downcutting at the Branch River Terraces, South Island, New Zealand. *Geological Society of America Bulletin*, 79, 545-556.

Lensen, G. J. (1976). Late Quaternary tectonic map of New Zealand, Hillersen & Renwick sheets. Wellington, New Zealand, Department of Scientific and Industrial Research.

Little, T. A., Grapes, R., and Berger, G. W. (1998). Late Quaternary strike slip on the eastern part of the Awatere fault, South Island, New Zealand. *Geological Society of America Bulletin*, 110(2), 127-148. Doi: 10.1130/0016-7606(1998)110<0127:Lqssot>2.3.Co;2.

Mason, D. P. M. (2004). *Neotectonics and Paleoseismicity of a Major Junction Between Two Strands of the Awatere Fault, South Island, New Zealand*. (Master of Science), Victoria University of Wellington, New Zealand.

Mason, D. P. M., and Little, T. A. (2006). Refined slip distribution and moment magnitude of the 1848 Marlborough earthquake, Awatere Fault, New Zealand. *New Zealand Journal of Geology and Geophysics*, 49(3), 375-382.

Mason, D. P. M., Little, T. A., and Van Dissen, R. J. (2006a) Refinements to the paleoseismic chronology of the eastern Awatere Fault from trenches near Upcot Saddle, Marlborough, New Zealand. *New Zealand Journal of Geology and Geophysics*, 49, 383-397.

Mason, D. P. M., Little, T. A., and Van Dissen, R. J. (2006). Rates of active faulting during late Quaternary fluvial terrace formation at Saxton River, Awatere Fault, New Zealand. *Geological Society of America Bulletin*, 118(11-12), 1431-1446. Doi: 10.1130/B25961.1.

McCalpin, J. P. (1996). Tectonic geomorphology and Holocene paleoseismicity of the Molesworth section of the Awatere fault, South Island, New Zealand. *New Zealand Journal of Geology and Geophysics*, 39(1), 33-50.

Rattenbury, M. S., Townsend, D. B., Johnston, M. R. (compilers). (2006). Geology of the Kaikoura area. Institute of Geological & Nuclear Sciences 1:250 000 geological map 13. 1 sheet + 70 p. Lower Hutt, New Zealand: GNS Science.

Zachariassen, J., Berryman, K., Langridge, R., Prentice, C., Rymer, M. Stirling, M., and Villamor, P. (2006). Timing of late Holocene surface rupture of the Wairau Fault, Marlborough, New Zealand. *New Zealand Journal of Geology and Geophysics*, 49, 159-174.

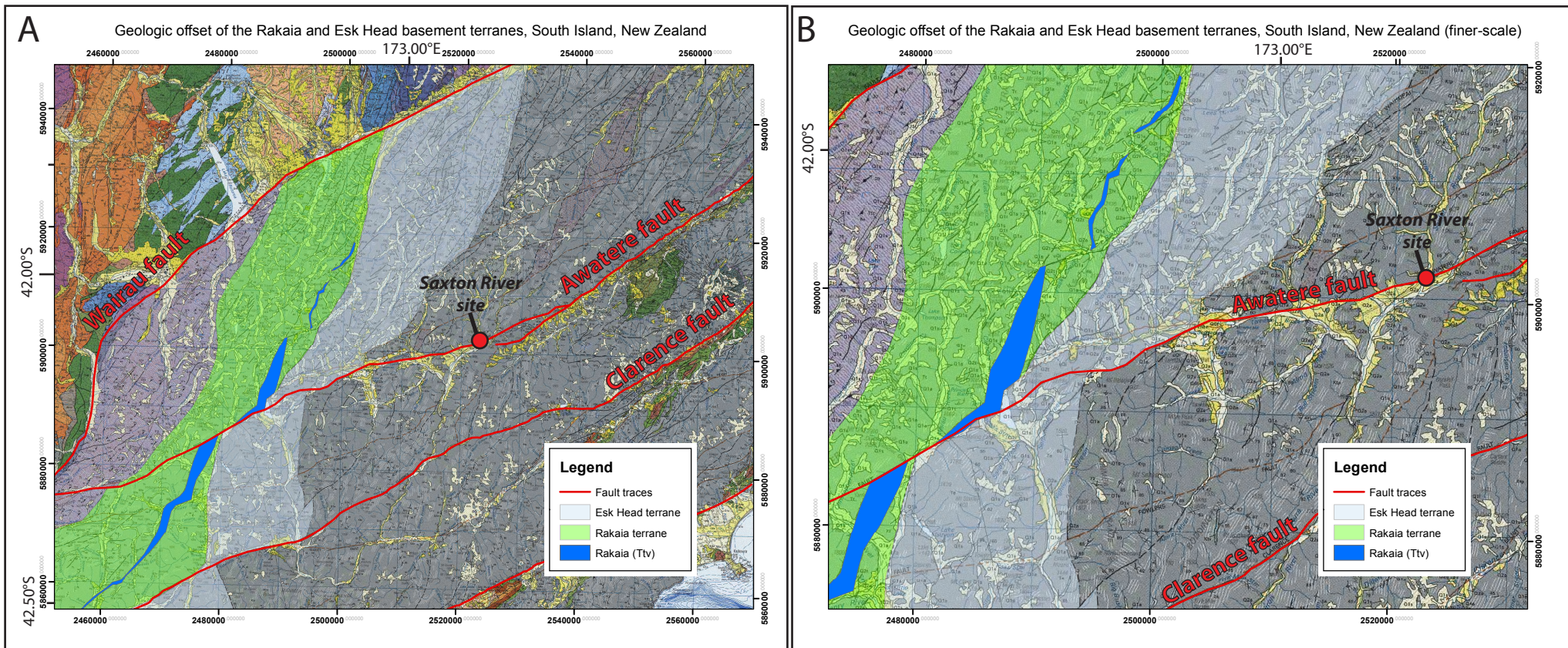


Figure DR1. Bedrock geology of the Marlborough fault system, northern South Island, New Zealand, showing the cumulative offset of the Awatere fault near the Saxton River site (modified from Rattenbury et al., 2006). Simplified traces of the Alpine-Wairau, Awatere, Clarence, and Hope faults are highlighted in red. (B) is a finer-scale map of the area shown in (A). Cumulative displacement of the Awatere fault is shown by offset of the Esk Head and Rakaia basement terranes. Although we suggest a maximum of 20 km of fault displacement on the Awatere fault, including 13 km of main strand slip and 5-7 km of distributed “drag folding”, as can be seen from the detail maps, much of the distributed off-Awatere right-lateral shear appears to be accommodated by several secondary fault strands to the N of the main Awatere fault. Maps are drawn using the New Zealand Map Grid Projection. Coordinates given in meters based on the New Zealand Map Grid using the Geodetic Datum 1949. Coordinates in decimal degrees are given for reference.

Reference: Rattenbury, M. S., Townsend, D. B., Johnston, M. R. (compilers). (2006). Geology of the Kaikoura area. Institute of Geological & Nuclear Sciences 1:250,000 geological map 13. 1 sheet + 70 p. Lower Hutt, New Zealand: GNS Science.

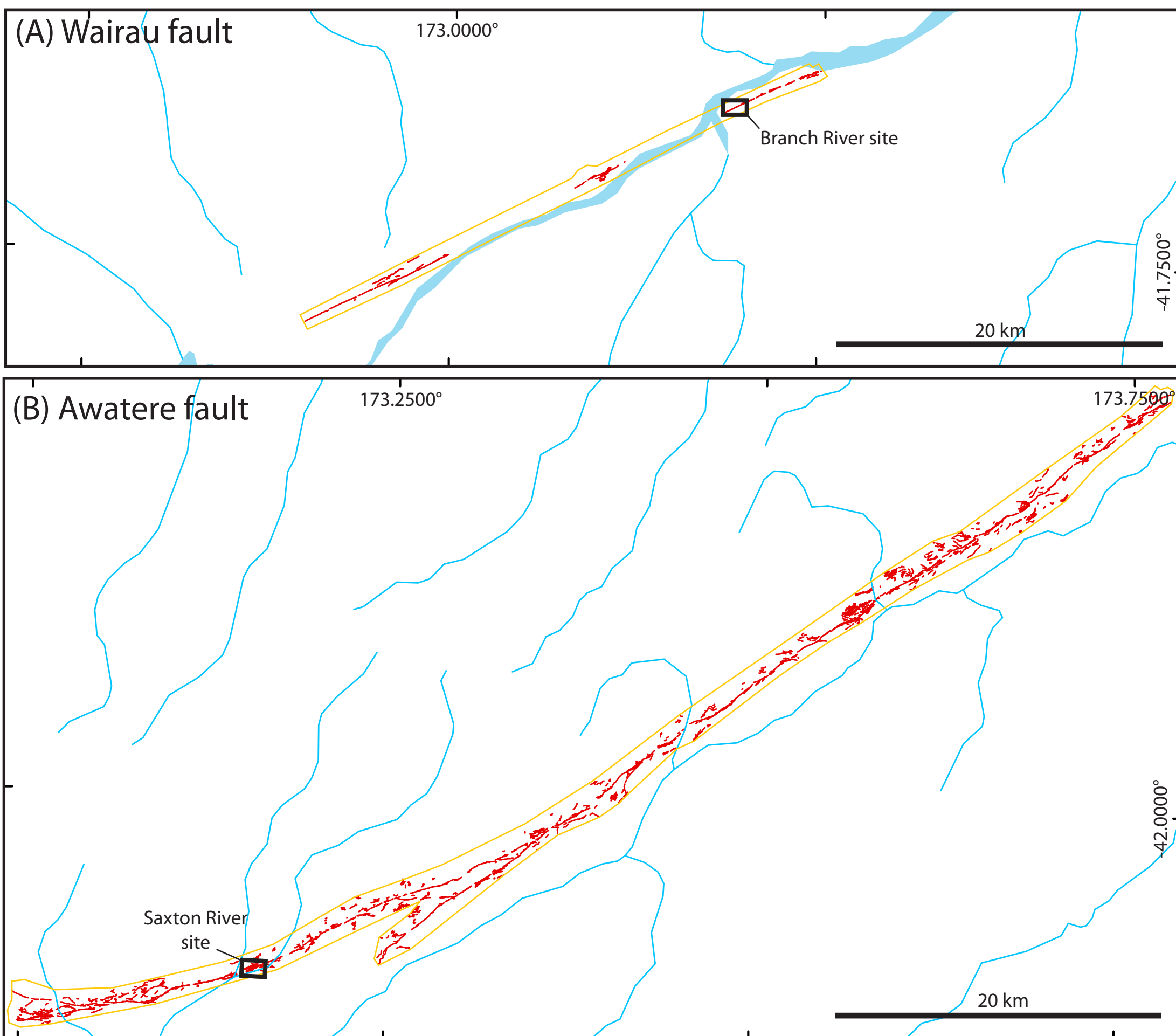


Figure DR2.

Fault traces and sackungen (red lines) mapped using the lidar data (acquisition outlined in orange). Gaps in mapped fault traces represent discontinuities in the fault trace, or places where erosion (e.g., by active rivers) has obliterated geomorphic evidence of the fault. The surface expression of the higher-displacement Wairau fault (A) is much structurally simpler than that of the lower-displacement Awatere fault (B) (Langridge et al., 2016). The surface deformation patterns expressed at the Branch River and Saxton River sites are generally representative of those observed along their respective faults.

Other examples of relatively structurally simple faulting occur at some locations along the Clarence and Hope faults to the south (which each have ~20 km of cumulative displacement [Little and Jones, 1998, and references therein]) as well as along the Awatere fault. Such examples may suggest the influence of other possible mechanisms locally controlling the surface expression of deformation, including topographic effects and variations in fault strike and dip (Barth et al., 2012; Khajavi et al., 2014). Such relatively structurally simple sites are not representative of broader deformation patterns along their respective faults.

References:

Barth, N. C., Toy, V. G., Langridge, R. M., and Norris, R. J. (2012). Scale dependence of oblique plate-boundary partitioning: New insights from LiDAR, central Alpine fault, New Zealand. *Lithosphere*, 4(5), 435-448. Doi: 10.1130/L201.1.

Khajavi, N., Quigley, M., and Langridge, R. M. (2014). Influence of topography and basement depth on surface rupture morphology revealed from LiDAR and field mapping, Hope Fault, New Zealand. *Tectonophysics*, 630, 265-284. Doi: 10.1016/j.tecto.2014.05.032.

Langridge, R. M., Ries, W. F., Litchfield, N. J., Villamor, P., Van Dissen, R. J., Barrell, D. J. A., Rattenbury, M. S., Heron, D. W., Townsend, D. B., Lee, J. A., Cox, S., Berryman, K. R., Nicol, A., and Stirling, M. (2016). The New Zealand active faults database: NZAFD250. Accepted to *New Zealand Journal of Geology and Geophysics*, 59(1).

Little, T. A., and Jones, A. (1998). Seven million years of strike-slip and related off-fault deformation, northeastern Marlborough fault system, South Island, New Zealand. *Tectonics*, 17(2), 285-302. Doi: 10.1029/97tc03148.

Table DR1. Offsets and ages of features and the Branch River and Saxton River sites

Wairau fault, Branch River site			Awatere fault, Saxton River site		
Feature	Horizontal offset (m) ¹	Age (ka) ²	Feature	Horizontal offset (m) ³	Age (ka) ⁴
Terrace A	55 ± 2	16 ± 2	Bedrock Spur	69 ± 5	> 14.5 ± 1.5
Terrace W	≥ 57 ± 2	14.7 ± 6.71	Terrace T1	69 ± 5	14.5 ± 1.5
Terrace B	57 ± 2	13.33 ± 2.47	Terrace T2	55 ± 6	6.7 ± 0.7
Terrace C	53 ± 2	12.07 ± 2.17	Terrace T3	32.5 ± 2.5	> 5.46 ± 0.77
Terrace D	38 ± 2	10.840 ± 1.89	Terrace T4	25 ± 2	5.46 ± 0.77
Terrace E	34 ± 2	10.840 ± 1.89	Terrace T5		
Terrace F	27 ± 2	6.72 ± 1.01	Terrace T6	9 ± 0.5	> 1.17 ± 0.11

¹ From Grenader et al. (2014).

² From Knuepfer (1992).

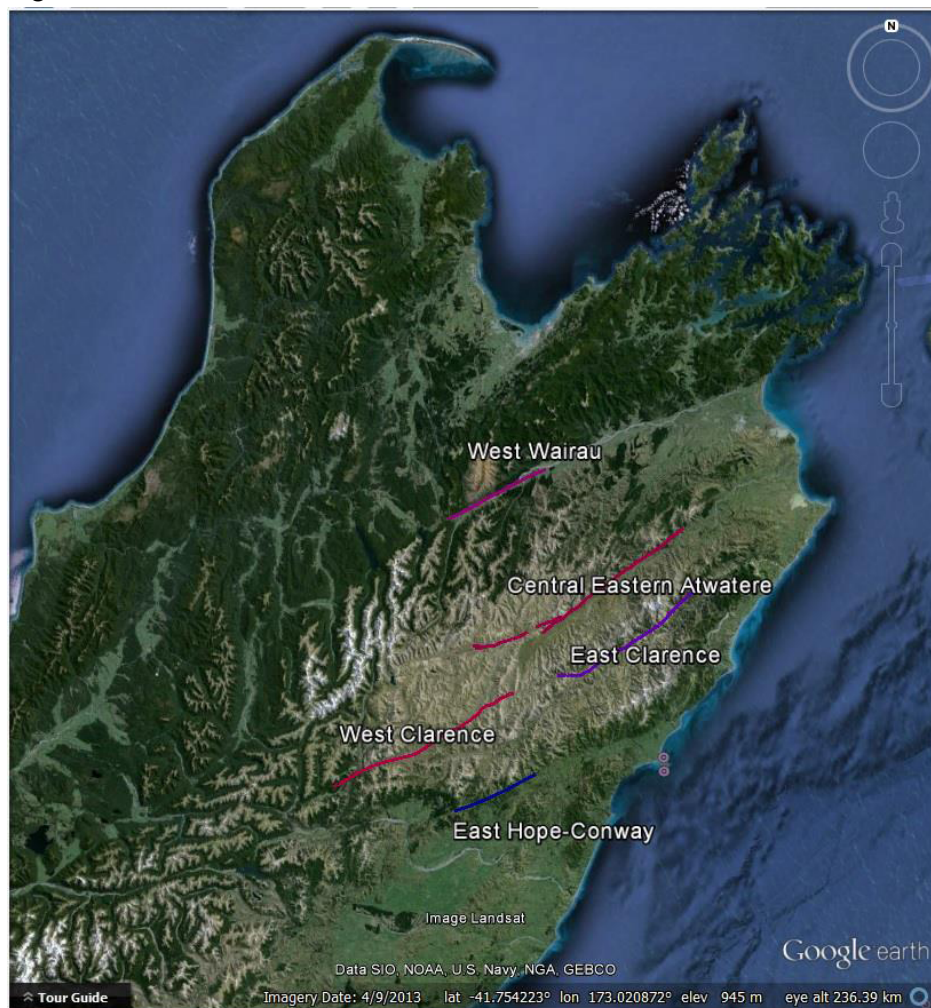
³ From Zinke et al. (2014a).

⁴ From Mason et al. (2006b) and references therein.

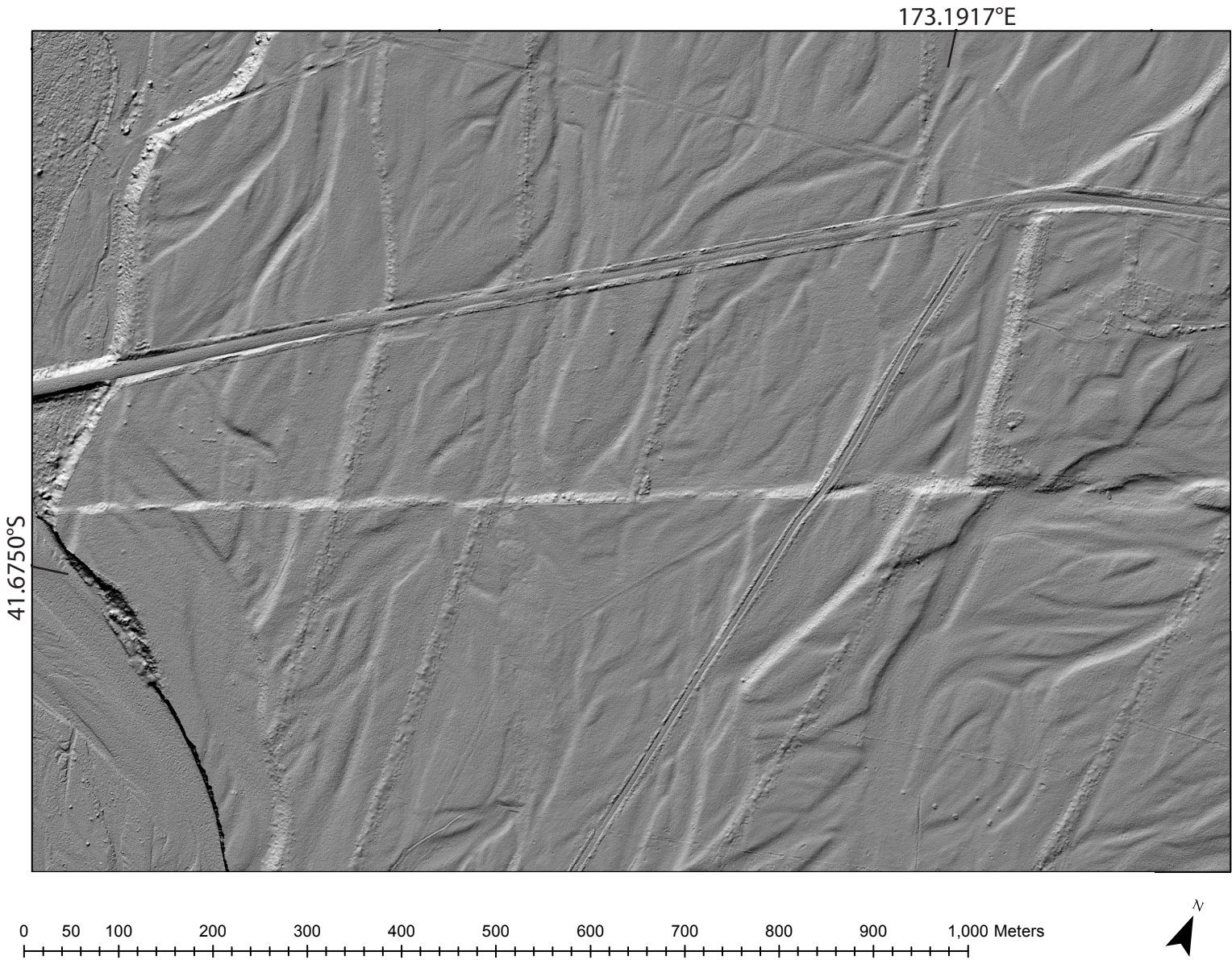
Lidar acquisition and processing report.

The lidar data were collected along a total of 254 km from five fault segments in the Marlborough Fault System, northern South Island, New Zealand (see figure below). Lidar swaths are (nominally) 1.2-km-wide, centered on each fault. The shot density is ≥ 12 shots/m². These data were collected as part of NSF Grant EAR-1321914 (to Dolan) for us by the US National Center for Airborne Laser Mapping (NCALM) and NZ Aerial Mapping using an Optech Gemini Aerial Laser Terrain Mapper (ALTM) serial number 06SEN195 mounted in a twin-engine Cessna 402B. Lidar was collected along the Wairau fault on 18 March 2014 with the sensor's pulse rate frequency (PRF) set to 100 kHz. Lidar was collected along the Awatere fault on 18–20 March 2014 using the same sensor, with PRF set to 125 kHz in Multi-Pulse Mode, which allows the laser-measured range to be twice as long as what the speed-of-light allows for a given altitude. The aircraft was nominally at 1400 m Above Ground Level (AGL) for lines flown at this setting. Ground point classification and bare-earth Digital Elevation Models (DEM) construction was performed by automated routines using TerraSolid TerraScan Version 14.008 software, a surfer kriging algorithm, Perl, Python & AML scripts. Bare-earth DEMs used in this study have a pixel size 0.33 m. Typical flight line height mismatch (Δz) in relatively flat areas is 0.02–0.05 m; in steep terrain, Δz increases to 0.05–0.12 m. Geomorphic features expressed by ≥ 20 cm of relief are discernable in the DEM, as determined by visual inspection. Features expressed by < 20 cm of relief will likely not be evident in the lidar, providing a minimum measurement threshold.

Figure DR3.



(A) Wairau fault, Branch River site – Hillshade DEM



(B) Awaterre fault, Saxton River site – Hillshade DEM

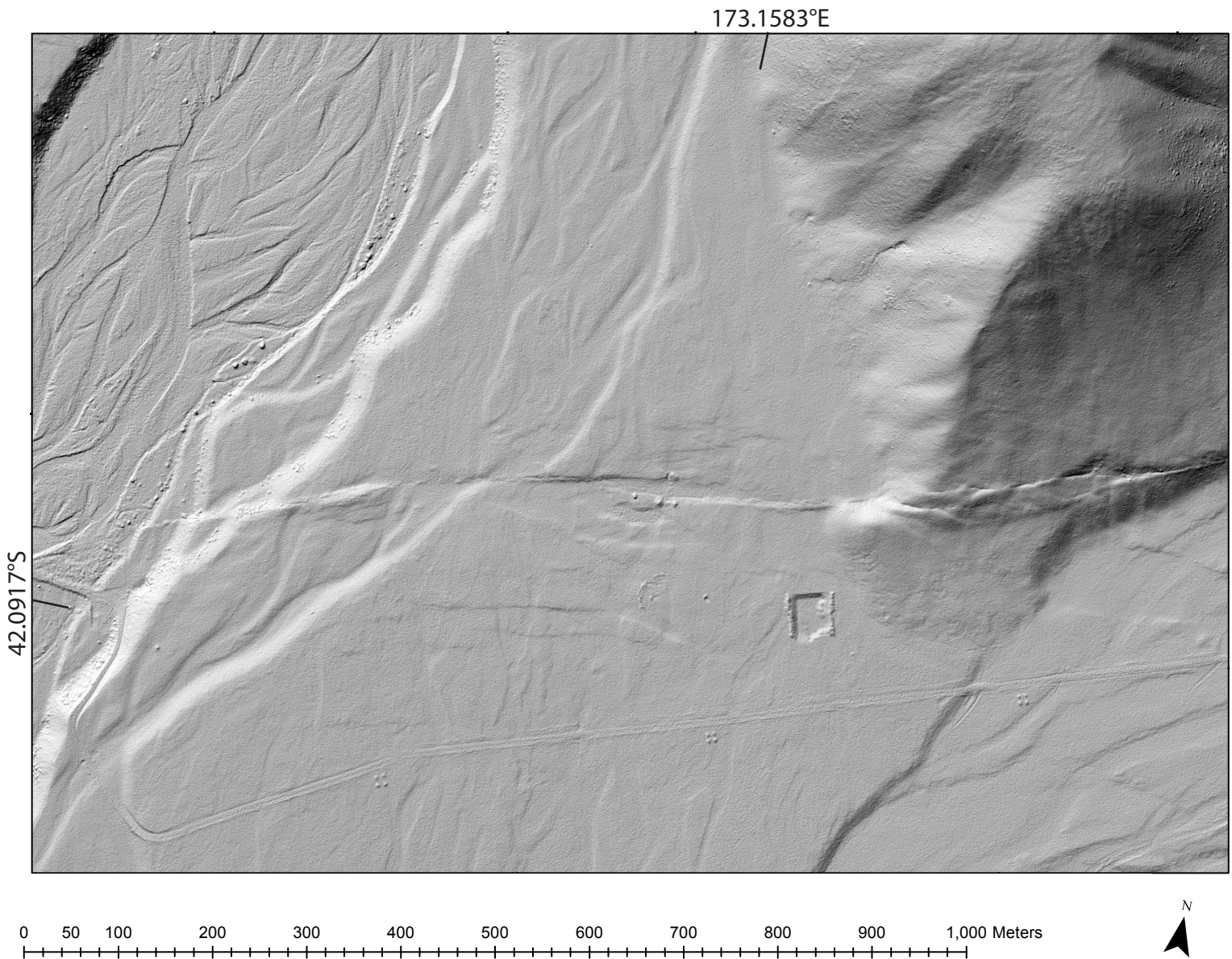


Figure DR4. Uninterpreted lidar hillshade digital elevation models of the Branch River (A) and Saxton River (B) sites along the Wairau and Awaterre faults, respectively. See supplemental material DR5 for lidar acquisition and processing details.

Coordinates in NZ grid.